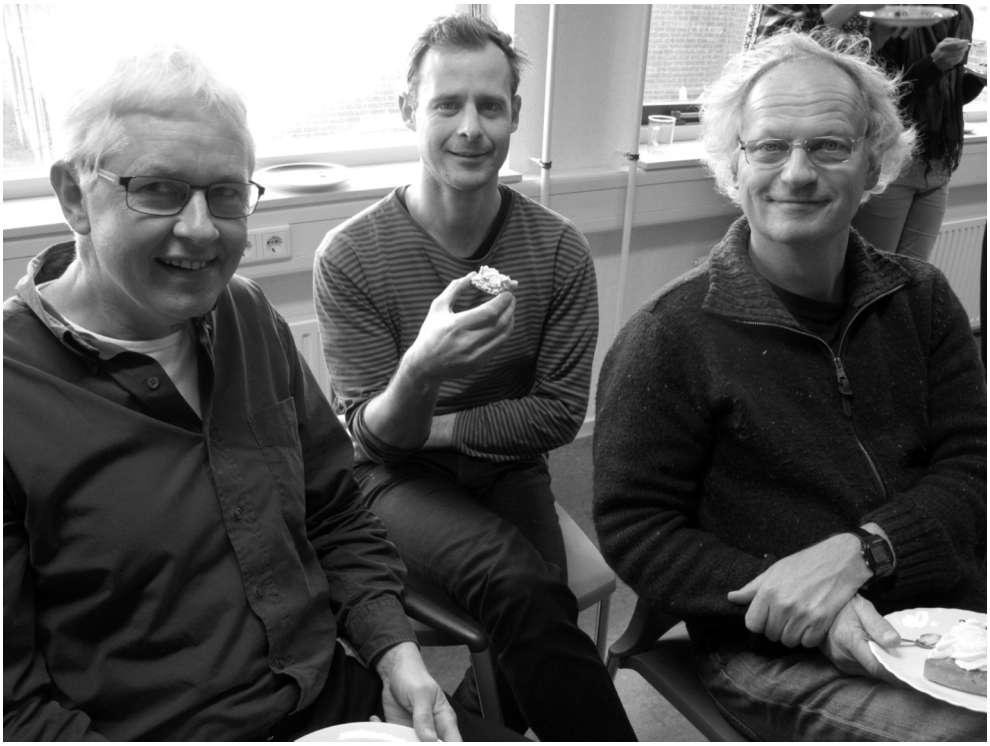

In the 1990s two young passionate scientists joined forces to get insight in a spectacular 'sixth-sense' organ in the tip of the bill of red knots *Calidris canutus* (Piersma et al. 1998). Now, 18 years after date, new insights in the foraging behaviour of red knots forced another young scientist to bring back together these scientists again.

Physical mechanism of remote touch

Leo R.M. Maas, Jimmy de Fouw and Theunis Piersma

ABSTRACT

A simplified physical and mathematical description is given of the mechanism employed by knots for remote detection of shells buried in soft sediments. This mechanism, which employs soil mechanical properties of wet sand, is described both for cases with or without a rhizome (sea grass root) layer below a surface mud layer. The presence of a rhizome layer reduces the permeability of that layer and consequently the knot's remote detection is.

Accepted for publication in *Animal Behaviour* as appendix

INTRODUCTION

Observation and experiments by Piersma et al. (1998) show that knots are able to sense the remote presence of shells (or pebbles), of some 1 cm diameter, in muddy sand. Knots can sense hard-shelled objects, buried over distances up to their bill length (approximately 3 cm). It is significant that their sensory capability fails in dry sand, in very liquid mud and, what is of particular interest here, when there is a rhizome mat shielding their prey (see main text for description).

Observation also shows that the tip of the knot's bill is (uniformly) covered with many tiny pressure sensors (Herbst corpuscles), whose threshold sensitivity (the minimally detectable pressure perturbation) and response time are unknown. We make a few assumptions concerning the bill that will be convenient in its physical modelling. We assume that the probing depth is very small, so that the probe, in its 'emitting' (forcing) mode, acts as a point-source of pressure fluctuations (located at the surface). This is also an accurate description when the emission is produced by a finite-sized spherical object, as long as the same mass-flux is affected. For the conical shape of the bill this should be modified at a later stage. During its detection mode, we assume that the bill penetrates to its true depth.

We first address, the following questions related to the pressure detection mechanism of probing bills and the specific demands posed on the mud and hydrodynamic environment, (1) What is the role of fluid in the mud, and why does the detection mechanism fail in dry or very liquid circumstances? (2) What is the role of the repetitive character of the probing? (Why is a single probe not sufficient?) (3) What is the role of the rhizomes layer on the detection mechanism?

Role of fluid in the mud layer

The probing of the bill will produce pressure variations in the mud. The properties of the medium at hand determine in what way it responds to pressure variations. In dry sandy sediments, for instance, pressure perturbations can, to a large extent, simply be supported by increased or decreased normal stresses of one sand grain upon another, without the necessity of having to yield. In other words, for tiny pressure perturbations, the sand, except in the very vicinity of the bill, acts as a solid. Fluids, on the other hand are unable to support pressure differences and always have to 'yield'. Consequently, they will immediately start to flow, thereby relaxing the pressure difference. Moreover, when forcing is at a liquid surface, the fluid will also respond by means of waves on that surface that will quickly remove the added energy towards infinity. In a muddy environment, however, there is enough water in the pores to produce a flow through it, while the absence of a free, liquid surface, eliminates the ability to remove energy by means of surface wave propagation. The pressure perturbation generated is, in other words, *trapped* in the forcing location.

The flow through pores is driven by pressure differences. The pores are tiny channels whose sides exert a drag on the flow along them. Indeed, side wall friction is the dominating mechanism which impedes the flow through the pores. The classical description of flow through mud is therefore one in which the pressure gradient is balanced by friction. Because of the complexity of the sand skeleton this is necessarily an empirical relation, known as Darcy's law (e.g. Sleath 1984):

$$\mathbf{u} = -k\nabla p,$$

where $\mathbf{u} = (u,v,w)$ is the fluid velocity in direction $x = (x,y,z)$-respectively, z pointing upwards, against gravity, p is the pressure, $\nabla = \partial/\partial x, \partial/\partial y, \partial/\partial z$ the gradient operator, and k an empirical constant proportional to the mud's permeability (proportional to the porosity of the mud), and inversely proportional to the viscosity of water. Although the pores may contain a substantial amount of air, which will make the aggregate of air and water within the pores susceptible to compression, we adopt the simplistic viewpoint that the pores are entirely filled with water, which is (nearly) incompressible. Hence the fluid is non-divergent:

$$\nabla \cdot \mathbf{u} = 0$$

(Accounting for the slight compressibility of water, or of the water-air mixture, would enable us to describe acoustic waves. For the range of probing frequencies given, however, these waves would have length scales of some hundreds of meters, far outside the range of interest of 5 cm, say.) Incompressibility of the pore water (adopted here) means that pressure variations will instantaneously be felt throughout this domain of interest. The probing bill will bodily displace sand and water and thus will also act as a mass source. This is modelled by introducing a source term at the right-hand side of the last equation. In the approximation that this is a point-source this will take the character of a Dirac delta function $\delta(\mathbf{x})$, a 'distribution', whose integral value only has physical significance representing the mass flux.

Role of repetitive probing

Assuming the permeability k to be spatially uniform, the previous two equations, with the addition of a point source, can be combined into a Poisson equation for the pressure:

$$\Delta p = \delta(\mathbf{x})\, e^{2\pi i f t} \qquad (1)$$

where the Laplacian operator $\Delta = d^2/dx^2 + d^2/dy^2 + d^2/dz^2$. Note that this only determines a spatial relationship for the pressure. Its time (t) dependence (introduced by the repetitive probing with frequency f) is parametric: $p \propto exp(2\pi i f t)$. Omitting the time-dependence (see below) the Poisson equation, (1), is solved by $p = 1/r$, where $r = (x^2 + y^2 + z^2)^{1/2}$ represents radial distance. The pressure in an infinite medium (for the

moment disregarding the upper surface), is thus simply inversely proportional to the distance to the source.

The knot's 'sixth sense' for remote detection of prey (Piersma et al 1998), employing repetitive, shallow probing, followed by a single deep probe in another direction, apparently uses the *build-up* of residual pressure near the knot's bill tip. Compaction may be responsible for such pressure build up. The periodic `shaking' of muddy sand by the probing action of the bill may explain the continuous increase in residual pore pressure. Each shake may lead to a (locally) more compact rearrangement of sand grains when the stirred-up sand grains fall back under the action of gravity. This process may lead to an associated increase of pore pressure and plays a dominant role, for example in liquefaction and the formation of quick sand (Sleath 1984). But the pressure field is not only changing in the vicinity of the bill. The residual (time-averaged) pressure pattern in the vicinity of a nearby shell will be affected as well, and in consequence this will in turn affect the pressure distribution around the bill. The intensity of this spatially-modified pressure pattern will increase at each successive cycle of the probing action, revealing the prey's location by making it, in every cycle more clearly 'visible'.

Response due to a rhizome layer with or without a shell

At the top of the rhizomes layer, situated at depth $z = -d$, the pressure, p, and the vertical velocity, $w = -kdp/dz$, perpendicular to that plane, have to be continuous. The permeability, k, of the lower rhizomes layer, k_l, is less than that of the upper mud layer, k_u. This is due to the decrease in the effective porosity of the sediment, and we assume that the rhizome root structure is so small that we can represent its presence in the form of a reduced effective permeability.

We next describe the response due to a localized pressure pulse induced by repetitive probing of a knot's bill, at $z = 0$. We consider three cases: first, the response in the absence of a shell, when a mud layer rests on top of a layer containing a rhizomes mat: second, the response to a shell in a mud layer without a rhizome mat, qualitatively discussed in Piersma et al (1998): third, the response to a shell buried in the lower layer containing the rhizomes mat. In the latter case we give particular attention to the pressure gradient sensed at the position of the knot's bill.

Response due to a rhizomes layer without a shell

Even in the absence of a prey (or stone) the change in permeability between a mud layer and a layer containing a seagrass root system (rhizomes mat) will affect the radial pressure distribution discussed above. Assuming the permeability to be constant within the rhizome layer, the pressure will again be governed by a Laplace equation. Hence the pressure will also be inversely proportional the radius, but with a reduced 'transmitted' amplitude T. The semipermeable interface between the mud and rhizome layers acts as a partial mirror. Therefore it augments the pressure field in the mud layer, where the knot senses the pressure difference relative to the uninhibited pressure field it knows it has been producing. This augmented field in the mud layer seems to come from a mirror

source situated in the rhizome layer at a distance from the interface at $z = -d$ equal to that of the source (the bill), at the surface and the interface. Therefore, the pressure is written as

$$p(x,y,z) = \begin{cases} p_u = \dfrac{1}{r_0} + \dfrac{R}{r_{-1}}, & z \in (-d, 0) \\ p_l = \dfrac{T}{r_0}, & z < -d \end{cases} \tag{2}$$

where $r_n \equiv (x^2 + y^2 + (z + Z_n)^2)^{1/2}$, denotes the distance with respect to source ($n = 0$) or images, located at $Z_n = -2nd$ for $n = (1,2,\ldots)$. At the interface between mud and rhizome layer, $z = -d$, we require continuity of the pressure $p_u = p_l$, (subscripts denoting upper (u) and lower (l) layer respectively), and also continuity of vertical velocity $k_u\, dp_u/d_z = k_l\, dp_l/d_l$. This determines reflection and transmission coefficients R and T in terms of $k = k_l/k_u < 1$:

$$R = \frac{1-k}{1+k}, \quad T = \frac{2}{1+k}. \tag{3}$$

The resulting pressure field is displayed in Fig. B6.1A.
In this computation, the top layer ($z > -d$) is treated as being of infinite extent. Therefore, the normal derivative of the pressure, dp/dz, and hence the vertical velocity, w, do not vanish at the water surface, $z = 0$. Figure B6.1A shows a weak inclination of the isobars relative to the vertical. The presence of the water surface, however, leads to a subsequent reflection of our virtual source at $z = -2d$, which creates a new mirror image above the water surface, at $z = 2d$. This mirror source, in turn, will produce a subsequent mirror source in the rhizomes layer at $z = -4d$ and so on, *ad infinitum*, and the pressure field due to this infinite sequence of source and mirror images is given by

$$p(x,y,z) = \begin{cases} p_u = \sum_{n=0}^{\infty} \left(\dfrac{R^n}{r_n} + \dfrac{R^{n+1}}{r_{-(n+1)}} \right), & z \in (-d, 0) \\ p_l = T \sum_{n=0}^{\infty} \dfrac{R^n}{r_n}, & z < -d \end{cases} \tag{4}$$

Taking for example, 50 mirror sources into account, the isobars indeed approach the water surface practically orthogonally (see Fig. B6.1B). When we subtract the initial pulse, we find the pressure perturbation as sensed by the knot (Fig. B.6.1C), which the knot may take to indicate the presence of a prey straight below its bill.

Perturbation due to a spherical shell

We now consider the impact of a shell (Piersma et al. 1998). For convenience this is assumed to be of spherical shape or radiusa <1, located at a radial distance $r = 1$ from the bill tip, at an oblique angle θ from the horizontal. In an infinitely extended mud layer, an appropriate array of image sources and sinks, located within the shell, will be able to generate a pressure and corresponding motion field such that the isobars are

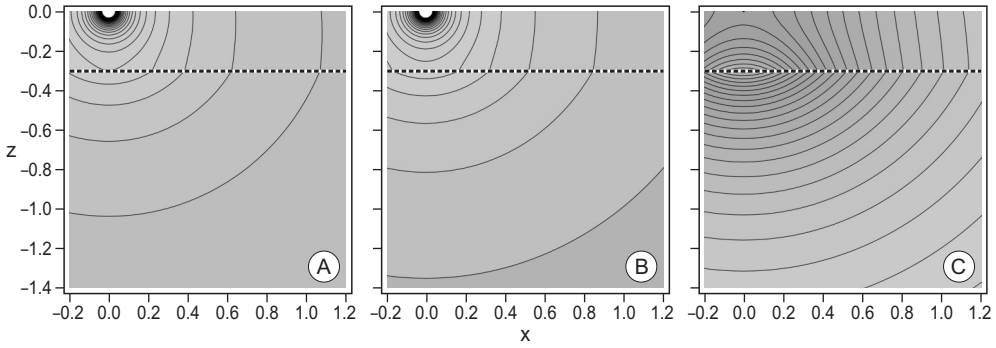

Figure B6.1 Rhizomes layer *without* shell: Pressure distribution, $p(\mathbf{x},z)$, for $k = 0.25$ taking in the summation (A) only the $n = 0$ term into account, or (B) up to $n = 50$. The top of the rhizomes layer is indicated by a dashed line. (C) Pressure perturbation, $p'(x,z) \equiv p - 1$, after eliminating the forced pulse at the source.

everywhere perpendicular, and thus the flow is parallel to the shell's boundary (Lamb 1932; p. 129), Fig. B6.2A. We let the source be at the origin and the centre of the shell define the x,z-plane. The residual pressure field is then most easily expressed in a coordinate system in which the x,z-coordinates, rotated to ξ,ζ-coordinates, with $\xi = -xs + zc$, $\zeta = xc + zs$, and $(s,c) \equiv (\sin\theta, \cos\theta)$, are such that the line connecting bill tip and prey is now defined as the new horizontal ξ-axis, and the line perpendicular to this as the new vertical ζ-axis. Then the residual pressure reads

$$p(x,y,z) = \frac{1}{r} + \frac{a}{\sqrt{(1-a^2-\zeta)^2+\rho^2}} + \frac{1}{a}\left[sinh^{-1}\left(\frac{1-a^2-\zeta}{\rho}\right) - sinh^{-1}\left(\frac{1-\zeta}{\rho}\right)\right],$$

where $\rho = (\xi^2 + y^2)^{1/2}$ is a horizontal radial coordinate. Subsequent figures show the $y = 0$ plane only (the plane containing bill tip and prey), in which the response is strongest. When we subtract the initial pulse, we find, however, that the isobars of the perturbation pressure field are not perpendicular to the water surface, $z = 0$, suggesting a flow through the surface (Fig. B6.2B) but this does not happen since the water surface is impenetrable. The surface acts as a reflector leading to another change in the pressure field. This is produced by a mirror image of the virtual sources invoked by the shell. Adding this contribution, the isobars are correctly perpendicular to the water surface (Fig. B6.2C) but at the bill tip, at the origin, $(x,z) = (0,0)$, this difference is sensed and informs the knot about the presence of a prey at $\theta = 60°$ relative to the horizontal, at a radial distance $r = 1$. Note that these image sources (located *above* the water surface) would require another perturbation pressure field in the vicinity of the shell, as the flow induced by that field would equally need to avoid penetrating the shell. In theory, an infinite sequence of virtual sources within the shell and above the water surface would be needed to exactly satisfy the impenetrability at shell and water surfaces. In practice, here and in what follows, we truncate this sequence after a few terms. When the shell is buried in a half-infinite

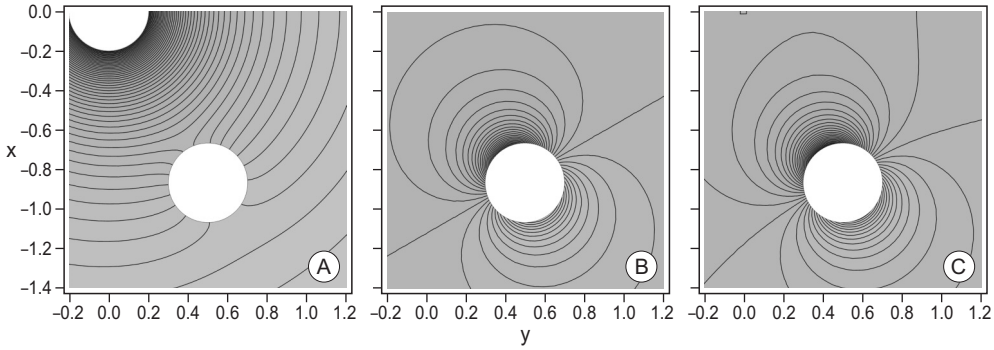

Figure B6.2 Shell without rhizomes layer: (A) Pressure distribution, $p(X,z)$, due to shell in infinitely deep mud layer without rhizomes. (B) Perturbation pressure, $p'(X,z)$ without the source. (C) As (B), but with reflecting water surface.

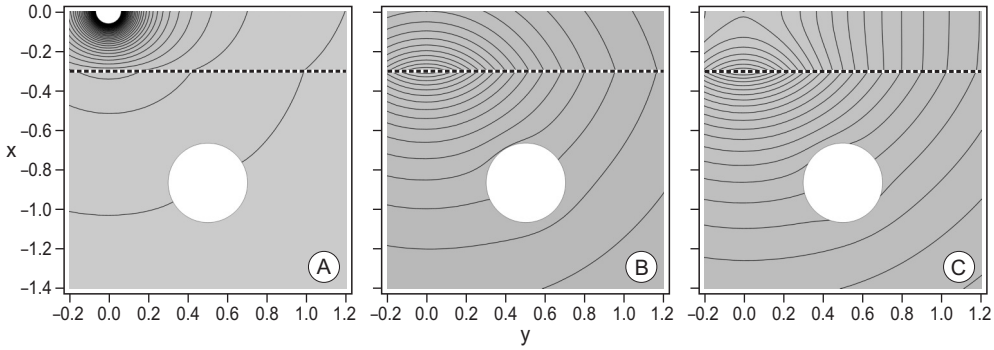

Figure B6.3 Shell within a rhizomes layer: (A) Pressure distribution , $p(X,z)$, due to shell in infinitely deep rhizomes layer located below mud layer. The interface between both layers is indicated by a dashed line. (B) Perturbation pressure $p'(X,z)$ without the source. (C) As (C), but with reflecting water surface.

rhizome layer of permeability $k = 0.25$ (leading to a reflection coefficient, $R = 0.6$) below a mud layer of depth $d = 0.3$, the rhizome mat changes the apparent strength of the source at the origin by a factor $T = 1 - R^2$. The change in the pressure field at the interface between mud and rhizome layer is clearly visible in a changing isobar inclination (Fig. B6.3A). Subtracting the influence of the source (Fig. B6.3B) shows that the pressure field in the mud layer no longer reveals the presence of the shell, even if we take the mirroring aspect of the surface into account (Fig. B6.3C). In both cases, the pressure difference is very nearly symmetric at the bill tip, at the origin $x = 0$, and no longer offers any clues on the direction (or distance) at which the prey can be found (compare Fig. B6.3C with Fig. B6.2C). In fact, while not *exactly* symmetric, it is clear that the pressure difference $p' = p - r^{-1}$ between the induced (p), and the imposed pressure r^{-1} – the difference sensed by the knot – is dominated by the direct reflection due to the presence of the

rhizome layer. This overwhelms the much weaker pressure difference due to the reflection by the shell and obscures the directional prey information.

Perturbation pressure gradient

The pressure difference below the top layer of depth d, of course, also depends on the actual change in permeability, k, due to a rhizome mat below, on shell size, a, and on shell angle, θ, relative to the horizontal. (We here assume the rhizome mat to be of semi-infinite extent). The strength of the pressure gradient as sensed by the knot's bill is estimated by taking only the influence of the rhizome layer and of a shell into account. Thus we discard the subsequent contribution consisting of mirror images due to the presence of the surface. The reason to do so is that the vertical component of the pressure gradient (proportional to the vertical velocity) vanishes at the surface. Since the knot's bill penetrates the mud layer over a few millimetres, the knot also senses this difference below the surface, where this component is not annihilated. In this way, the pressure gradient at the origin, $(x,y) = (0,0)$, affected by the sea grass roots and a shell, contains apart from its magnitude, directional information, ϕ, which can be computed analytically. It is given by

$$-\nabla p' \equiv |\nabla p'|(\cos\phi, \sin\phi) = (1-R^2)\frac{a^3}{(1-a^2)^2}(\cos\theta, \sin\theta) + \left(0, \frac{R}{4d^2}\right).$$

Without a rhizome layer, the permeability ratio $k = 1$, and thus there is no reflection, $R = 0$, and the pressure gradient decreases with decreasing shell size, a. In the vertical plane this points towards the shell position, $\phi = \theta$. With a rhizome layer, but *without* a shell ($a = 0$), the perturbation pressure gradient points simply downwards, towards the image source. This may falsely suggest the presence of a shell at a depth $2d$, twice the thickness of the sediment layer on top. For a single depth $d = 0.3$ and shell diameter $a = 0.2$, the

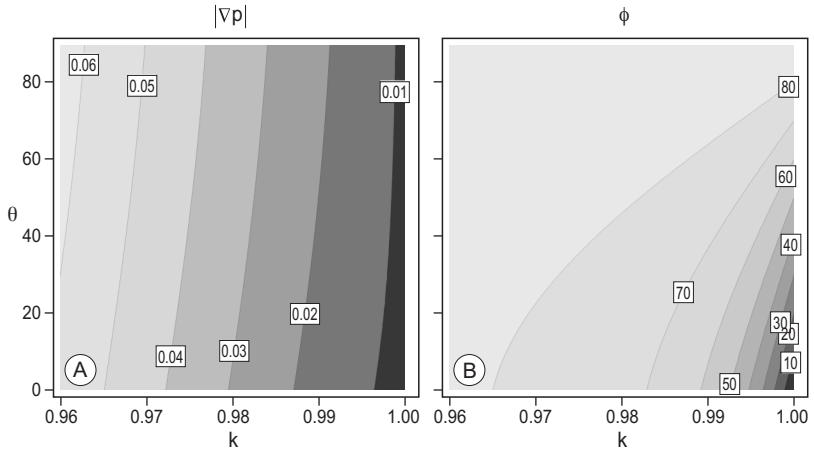

Figure B6.4 Perturbation pressure gradient sensed at the bill tip ($x = (0,0,0)$): (A) magnitude, $|\nabla p|$, (dimensionless units and colours) and (B) direction, ϕ, (labelled contours in degrees and colour) as a function of shell angle to the horizontal, θ, and of permeability ratio, k.

magnitude $|\nabla p'|$ and direction ϕ, relative to the horizontal, are displayed in Figures B6.4A, B. The figure reveals that even under a small 4% drop of permeability in the lower rhizomes layer, the perturbation pressure gradient magnitude increases by a factor of 10 (see the left side of Fig. B6.4A). Obviously, the contribution to the perturbation pressure by the shell is dwarfed by that due to the virtual image source. Most significantly, the angular information on the position of the shell is almost lost, since $\phi \approx 90^\circ$ for any shell direction θ (meaning the knot believes the prey to be buried vertically below the bill). This sensitive dependence on permeability remains present for other surface layer depths, d, and shell diameters, a.